


 Cite this: *RSC Adv.*, 2022, 12, 23311

# Effects of different tempering temperatures on the properties of industrial sheet margarine†

 Houbin Gao,<sup>a</sup> Wei Gao,<sup>b</sup> Xiaomin Yang,<sup>c</sup> Yuanfa Liu<sup>b,\*d</sup> and Zhouping Wang<sup>\*ae</sup>

Tempering is the final step in Industrial Sheet Margarine (ISM) production, which has a substantial influence on the structure and application characteristics. There are limited reports on how the tempering process affects the ductility and application characteristics of ISM at an industrial production scale. Herein, we investigated the physicochemical properties and ductility of the ISM made from interesterification and non-interesterification fat at various tempering temperatures (10, 15, 20, 25, and 30 °C) for 5 days. By analyzing the triacylglycerol (TAG) compositions, polymorphism, thermal behavior and hardness of ISMs under different formulations and tempering conditions, the interaction between the physicochemical parameters and the application properties such as bending and sheeting abilities was elucidated. The results showed that low tempering temperatures (10 °C and 15 °C) led to higher hardness (>700 g) while high tempering temperature (30 °C) promoted polymorph transition ( $\beta' \rightarrow \beta$ ), further directing to poor crystallization behavior, poor plasticity and malleability. Products tempered at 20 °C and 25 °C exhibited optimal ductility properties. These findings provided practical guidance to improve the ductility of sheet margarine in industrial level production.

 Received 29th June 2022  
 Accepted 5th August 2022

DOI: 10.1039/d2ra03999k

[rsc.li/rsc-advances](http://rsc.li/rsc-advances)

## 1 Introduction

Industrial Sheet Margarine (ISM), commonly known as puff pastry margarine or roll-in margarine, is a highly plastic structured fat and is widely utilized in the production of puff pastries to give the desired layers and crispy mouth feel of the final baked products.<sup>1,2</sup> It is a water-in-oil (W/O) emulsified system in which the solid fat portion provides the crystal network to stabilize the liquid oil and water in the spaces within the emulsion network in the presence of emulsifiers.<sup>2,3</sup> Traditionally, pure plant-based ISMs are usually based on palm oil, soybean oil, rapeseed oil, or their hydrogenated fats, and animal-based ISMs are mainly made using animal fats such as tallow, anhydrous milk fat, and also vegetable oils.<sup>4</sup>

The production of ISM mainly includes blending, emulsifying, chilling, kneading, resting tube, molding, and tempering. Temperature is the most important parameter in the process of

ISM production because it has a significant influence on the crystal form and the strength of the crystal network in specialty fat formula. Tempering is a crucial process to ensure the stability and quality of final products. Generally, crystal polymorphic properties are highly depended on the temperature of crystallization and the rate of cooling. With regards to crystallization temperature, for palm oil, crystallization at 18 °C leads to the formation of  $\alpha$ -type crystal, while crystallization at 22 °C,  $\beta'$  type crystal is formed from the melted fat.<sup>4</sup> For anhydrous milk fat,  $\alpha$ -type crystal is easily formed in the process of rapid cooling, and a transformation of  $\alpha$  to  $\beta'$  type crystal takes place followed by the kneading process. However,  $\beta'$  crystals can be formed directly at low cooling rates.<sup>5</sup> This is because the supercooling does not allow sufficient time for the triglyceride molecules to align their crystal structure and thus form a low-stability crystal form. In addition, the cooling rate also affects the size of crystals. For example, large crystals are usually formed at a low cooling rate while small crystals are formed at a fast cooling rate.<sup>6,7</sup>

Tempering refers to the process of storing a product after packaging at a specific temperature for a period of time (normally 1–10 days).<sup>8</sup> During tempering, crystal transformation takes place in which the unstable crystal mass is partially melted firstly, then recrystallized to a more stable crystal morphology.<sup>7</sup> The low melting constituents tend to recrystallize into more stable crystal form with a higher melting point. Therefore, temperature and time can affect the crystallization stability and consistency and further affect the application properties of products. Drelon *et al.* performed oscillatory

<sup>a</sup>State Key Laboratory of Food Science and Technology, School of Food Science and Technology, Jiangnan University, 1800 Lihu Road, Wuxi 214122, Jiangsu, People's Republic of China. E-mail: wangzp@jiangnan.edu.cn; Tel: +86-15951581339

<sup>b</sup>School of Materials Science and Engineering, Tianjin University of Technology, Tianjin, 300384, China. E-mail: gaoweijut@126.com

<sup>c</sup>Wilmar (shanghai) Biotechnology Research & Development Center Co., Ltd, Shanghai, 200137, China. E-mail: yangxiaomin@cn.wilmar-intl.com

<sup>d</sup>School of Food Science and Technology, Jiangnan University, Wuxi 214122, China. E-mail: yfliu@jiangnan.edu.cn; Fax: +86-0510-85876799; Tel: +86-0510-85876799

<sup>e</sup>Key Laboratory of Meat Processing of Sichuan, Chengdu University, Chengdu, 610106, China

† Electronic supplementary information (ESI) available. See <https://doi.org/10.1039/d2ra03999k>



rheological measurements of AMF-based cream during and after tempering treatment at 15–30 °C, results indicated that the fat network of tempered creams was more rigid and resulted in enhanced structural stability,<sup>7</sup> but the emulsion system of dairy was completely different from that of ISM. Moziar *et al.* studied physical changes of partially hydrogenated contained shortening which manufactured in two votators pilot in different tempering conditions and came to the conclusion that the hardness of shortening was significantly increased at 10 °C tempering but significantly decreased at 30 °C tempering.<sup>8</sup> Nevertheless, partially hydrogenated fats were rarely used in ISM due to the TFA issue. Zhang *et al.* evaluated on the physical behavior of palm oil-based margarine tempered at 20, 25 and 30 °C and concluded that the samples tempered at 20 °C had poor spreadability and post-hardening occurred during storage. Though the spreadability of the samples was best at 30 °C, the samples were in general too soft with also poor thermal stability leading to grainy texture.<sup>9</sup>

Although a few previous studies were reported, either the formulations designed were not consistent with commercial products or the samples were prepared using a laboratory-scale pilot machine. Their formulations and processing were quite different from those of commercial ISM products. Therefore, the conclusions mentioned above, when applied to actual industrial production, can have a certain help to the product quality, but it can't fundamentally reduce defective rate of products caused by poor ductility. To the best of our knowledge, insufficient attention has been paid to evaluate the impact of tempering on the physical–chemical and application properties of ISM, such as the structure of the fat crystal network, plasticity, hardness, and ductility. The purpose of this paper is to systematic investigate the impacts of tempering on the properties and operational functionalities of ISM and to elaborate the interaction between the physicochemical parameters and the application properties. Different tempering temperatures (10 °C, 15 °C, 20 °C, 25 °C and 30 °C) were applied for different ISMs, which were formulated with and without interesterification oil in the production system. NMR, DSC, PLM, XRD, texture analysis, bending, and sheeting techniques were applied to evaluate the changes in crystallization behavior, thermal behavior, physicochemical properties, and application characteristics of ISM. Further, we also aimed to provide theoretical guidance for practical industrial production.

## 2 Materials and methods

### 2.1. Materials

Palm Stearin (ST, Iodine Value (IV) 33–35 g I<sub>2</sub>/100 g), Palm Kernel Olein (PKOL, IV 22–24 g I<sub>2</sub>/100 g), and soybean oil (SBO, IV 128–131 g I<sub>2</sub>/100 g) were provided by Kerry Grain and Oil Co. Ltd (Tianjin, China). Monoacylglycerides (MAG) and lecithin were procured from Danisco (China) Co., Ltd and Qinhuangdao Golden Sea Grain and Oil Co., respectively. Potassium sorbate was from Daicel Nanning Food Ingredients Co. Ltd. β-Carotene and butter flavors were from BASF (China) and Givaudan (Shanghai), respectively. Sodium methylate and citric acid were from Aladdin Reagent (Shanghai) Co. Ltd. *N*-Hexane (>99.5%)

and isopropanol were chromatographic pure. Potassium hydroxide and methanol were analytical pure, they were all from Aladdin Reagent (Shanghai) Co. Ltd.

### 2.2. Sample preparation

**2.2.1. Chemical interesterification (CIE) of oil blends.** Pre-weighed ST, PKOL, and SBO were proportionally pumped into the reaction tank which was jacketed for heating and cooling with steam and water, respectively. The oils were well mixed for 15 min and heated to 105 °C with stirring and vacuum for 30 min to remove the moisture traces. Next, sodium methylate (0.1 wt% of the oil mass) was discharged into the tank due to the vacuum condition and interesterification proceeded under vacuum (~3 torr) and lasted for 0.5 h. At the end of the reaction, the vacuum was released first, then a solution of citric acid (10% concentration) was added to stop the reaction. Hot water was added to wash the blends and subsequently removed by centrifugation. The inter-esterified oil was dried (at 105 °C for 0.5 h under vacuum of 5 torr), bleached (performed at 105 °C for 25 min with addition of 1.0 wt% bleaching earth under vacuum of 5 torr then filtrated at 70 °C), and deodorized (at 250 °C, vacuum of 3 torr for 1.0 h) for sheet margarine production.

**2.2.2 Production of industrial sheet argarine.** The commercialized formulations (coded A and B) presented in Table 1, included fats (80%), water (16%), emulsifiers (1% MAG and 0.5% soybean lecithin), salt, preservative, colorant, and flavor. The fat blends were designed based on four considerations all linked to industrial final application of ISM: (i) a flat SFC curve for wider operational temperature range, a sufficient level of SFC at 30 °C (above 20%); (ii) a low solid fat content at 40 °C (less than 6%) for good mouth melting profile; (iii) a saturated fatty acids level lower than 65% (butter) for healthy concern; (iv) cost efficiency. The addition of 15% PKOL can improve sharp melting profile and accelerate the crystallization with minimal cost increasing. While ensuring sufficient level of SFC, 35% SBO was added to reduce the content of saturated fatty acids as much as possible.

Initially, all the emulsifiers were added to the oil base to obtain the oil phase, then the aqueous phase was pumped into the oil phase tank, and mixed well for 30 min to produce

Table 1 Commercial formulations of A and B

Ingredients (%)	A	B
ST	16.18	16.18
50ST + 15PKOL + 35SBO	64.71	—
CIE (50ST + 15PKOL + 35SBO)	—	64.71
Subtotal fat blends	80.89	80.89
Monoacylglyceride (MAG)	1.00	1.00
Lecithin	0.50	0.50
β-Carotene	0.004	0.004
Butter flavor	0.02	0.02
Water	16.00	16.00
Salt	1.50	1.50
Potassium sorbate	0.09	0.09
Subtotal additives	19.11	19.11
Total	100	100



a stable emulsion. Finally,  $\beta$ -carotene and flavors were added to the emulsion 15 min prior to cooling.

The ISMs were manufactured in a margarine plant using a SPX Nexus 244 LC system configured with 4 cooling units (named C1, C2, C3, and C4), one pin machine (P1, volume 100 L), and one resting tube (RT). The pipe connection was C1–C2–P1–C3–C4–RT, the reason to place P1 between C2 and C3 was to provide enough time for the supercooling emulsion to crystallize after intensive chilled by C1 and C2. The flow rate was 2500 L h<sup>-1</sup>, and the rotational speeds were 490 rpm and 100 rpm for cooling units and pins, respectively. The temperatures of the chilling media (CO<sub>2</sub>) for C1, C2, C3, and C4 were set at -5, -5, -10, and -10 °C, respectively. The inlet temperature of the emulsion was about 55 ± 2 °C after pasteurization, and the outlet temperature of the product was about 14 ± 2 °C. The product was packed in 1 kg per sheet covered with two PE films, and 10 sheets were packed in one carton box. Once manufactured, samples of the two different recipes were immediately tempered at 10, 15, 20, 25, and 30 °C for 5 days with 2 boxes at each temperature. After tempering, all samples were stored at 5 ± 1 °C for further evaluation. The configuration and process of production were shown in ESI Fig. S1†

### 2.3. Fatty acid (FA) and triacylglycerol (TAG) composition

Fatty acid composition of the fat phases of samples A and B were determined according to the AOCS method Ce 1f-96 as reported by Adhikari & Hu (Adhikari & Hu, 2012). It was done by Gas Chromatography (GC) analysis of FAME performed by an Agilent 7820A GC system equipped with a Agilent GC capillary column (CP-sil 88 100 m × 0.25 mm; Agilent Technologies Inc., Middelburg, Netherlands). The preparation of fatty acid methyl ester (FAME) was referred to AOCS CE 2-66 standard.<sup>10</sup> Weigh 0.5–1.0 g in a 15 mL sample bottle. 5 mL *n*-hexane and 3 mL 0.5 mol mL<sup>-1</sup> KOH–CH<sub>3</sub>OH solution were added, covered and mixed, and then heated in a 60 °C water bath for 0.5 h. Immediately after removal, centrifuge was centrifuged at 4500 rpm for 5 min, and the supernatant was taken for GC analysis. GC analysis of FAME was performed with a flame ionization detector (FID) and chromatographic column (Agilent CP-sil 88, 50 m × 0.25 mm × 0.2 μm). The injection and detector temperatures were 250 and 280 °C respectively. The flow rate of hydrogen and air was 40 mL min<sup>-1</sup>, and 400 mL min<sup>-1</sup> respectively, and the injection volume was 0.2 μL. The identification of FAME was based on the external standards using commercial reference fatty acids. All determinations were performed in three replicates and the average value was reported.

Triacylglycerol (TAG) compositions of samples were analyzed by ultra-performance convergence chromatography (UPC<sup>2</sup>) combined with a quadrupole time-of-flight mass spectrometry (Q-TOF-MS) and the method referred to the literature.<sup>11</sup> Before loading, 1 g of sample was dissolved in 10 mL of *n*-hexane/isopropanol solvent (7 : 3, v/v), and then filtered through a cartridge filter (0.22 μm). The qualitative analysis was performed at 50 °C by the Waters Acquity UPC2 system equipped with an Acquity UPC2 BEH 2-EP column (150 mm × 3.0 mm

i.d.; 1.7 μm; Waters, Milford, MA, USA). The mobile phase A was CO<sub>2</sub>, the mobile phase B was acetonitrile: ethanol 1 : 1 (v/v), and gradient elution B was conducted as follows: 0.2%, 0.7%, 0.8%, 1.2% at 0, 5, 10, 15 and 20 min respectively. The back pressure was set at 1600 psi. 1.0 μL of each sample was injected with a flow rate of 1.2 mL min<sup>-1</sup>. The chemical constituents of sample were analyzed using a Waters Xevo G2-S Q-TOF mass spectrometer (Milford, MA, USA). The data acquisition range was *m/z* 440–1000 in a positive ion electrospray ionization (ESI) mode. The voltages of capillary, the cone and the source offset were 2.5 kV, 40.0 V and 80 V respectively. The temperatures of source and desolvation are 120 °C and 500 °C with the desolvation gas flow rate of 900.0 L h<sup>-1</sup> and the cone gas flow 80.0 L h<sup>-1</sup>. To collect data in TOF MS experiments, two separate scan functions were programmed for the MS acquisition method. The scan time for each function was set at 0.3 s. Data were acquired and analyzed with Waters MassLynx v4.1 software. The measurements were performed in triplicates.

### 2.4. Solid fat content (SFC)

SFC of oil base was measured according to the AOCS method Cd 16-93b on a nuclear magnetic resonance (NMR) analyzer (Bruker minispec MQ 20, Germany). About 3.0 g melted oil sample was put into a NMR tube and three NMR tubes for each sample at each temperature. Then the NMR tubes were put in a 60 °C water bath for 30 min to ensure the complete melt of the oil samples. Then, the tubes were moved to a 0 °C water bath and placed for 60 min to crystallize the oil samples. Lastly, the oil sample tubes were placed in the water bath at 10, 20, 25, 30, 35, and 40 °C for 30 min prior to SFC determination. All determinations were performed in triplicate and results were reported as average of three repetitions.

SFC of the solid sheet margarine was determined by plunging about 3.0 g margarine into NMR tubes using an specific designed plunger.<sup>12</sup> The NMR tubes were placed at incubators of 10 °C and 20 °C for 24 hours, respectively, followed by SFC determination using NMR analyzer. Each sample was measured in three replicates and results are reported as average of three repetitions.

### 2.5. Crystal structure observation

The characterization of margarine crystallization was determined using Polarized Light Microscopy (PLM) with a Nikon Eclipse E 400 microscope. A proper amount of sample was taken by capillary tube and pressed on the glass slide to form a transparent sheet, which was observed by polarized light microscope with magnification of 50 × 10, and further processed using a random image processing software.

### 2.6 Thermal behavior

The thermal properties of the ISMs were measured using Differential Scanning Calorimeter (DSC, TA Q2000). 4–5 mg samples were accurately weighed into an empty aluminum crucible. Under the atmosphere of 50 mL min<sup>-1</sup> nitrogen, the test temperature procedure was set as follows: isothermal holding at 5 °C for 5 min, heating from 5 to 80 °C at 5 °C min<sup>-1</sup>.



## 2.7 The rates of crystallization

Crystallization rates were measured using NMR analyzer to obtain the curves of SFC vs. time. About 3.0 g melted oil sample was put in a NMR tube followed by heating at 60 °C water bath for 30 min to ensure the complete melt of the oil sample. Then, the tubes were transferred to a water bath at different isothermal crystallization temperatures (5, 10, 15, and 20 °C), and the SFC was detected at an interval of 2 min for 40 min in terms of the literature method.<sup>13</sup>

## 2.8. Polymorphism identified by X-ray diffraction (XRD)

The polymorphism of each margarine was investigated using an X-ray diffractometer (X'Pert PRO, analytical B.V., Holland) ( $\lambda$  Cu = 1.54 Å, 40 kV, 40 mA). The X-ray diffraction patterns were recorded at 25 °C in  $2\theta$  range from 2° to 30° and the scan speed was 2° per min. The polymorphism was determined according to the short spacings. There are  $\alpha$  form at 4.15 Å,  $\beta'$  form at 4.2–4.3 and 3.7–4.0 Å, and  $\beta$  form at 4.6 Å.<sup>14</sup> Measurements were performed for each product tempered at different temperatures.

## 2.9. Hardness and texture

The hardness of each margarine was measured by a Texture Analyzer (SMS TA. XT 2i/5, Stable Micro Systems, Surrey, UK). The penetration distance was 10 mm with a P/6 probe. The maximum penetration force was recorded and presented in g to represent the value of hardness.

Samples were placed in 10, 15, 20, and 25 °C incubators for 24 hours before measurement to ensure the samples were at a constant specific temperature. Results are reported as means of triplicates.

## 2.10. Bending and sheeting test

Samples were placed in 10 °C, 15 °C, and 20 °C incubators for 24 hours and bent to 90° to observe the fracture of the samples. The sheeting test was carried out using a Rondo sheeter (SSO 605, Switzerland). Samples were taken out from the incubator and sheeted down in the process of 20 mm → 15 mm → 10 mm → 6 mm → 4 mm gradually. The consistency of the margarine belt was then observed.

# 3 Results and discussion

## 3.1 FA and TAG composition

FA and TAG composition greatly influences crystalline network and physical properties.<sup>15</sup> Table 2 presented the FA composition and quantity in sample A and B. There were no differences ( $p > 0.05$ ) due to the similarity of base stock. The major FA component in A and B was palmitic acid (C16:0) with 41.21%, and 41.40% respectively, which mainly came from palm oil. There was high content of polyunsaturated FAs (PUFA) with 18.29% and 18.20% linoleic acid (C18:2), and 1.70% and 1.57% linolenic acid (C18:3) for A and B, respectively, which were mainly from SBO. Compared to saturated fatty acid (SFA) content (about 65%) of butter, sample A and B containing lower SFA (about 53%) match the SFA-reducing trend.<sup>16–18</sup> PKOL was widely used in margarine

Table 2 Fatty acid composition (%) of samples A and B<sup>a,b</sup>

	A	B
C8:0	0.51 ± 0.03	0.50 ± 0.03
C10:0	0.55 ± 0.02	0.57 ± 0.01
C12:0	4.01 ± 0.15	3.88 ± 0.05
C14:0	2.14 ± 0.63	2.13 ± 0.02
C16:0	41.21 ± 1.04	41.40 ± 1.03
C18:0	4.77 ± 0.19	4.74 ± 0.23
C18:1T	0.12 ± 0.01	0.13 ± 0.01
C18:1	27.68 ± 0.87	27.83 ± 0.74
C18:2T	0.19 ± 0.01	0.25 ± 0.01
C18:2	18.29 ± 0.78	18.20 ± 0.83
C18:3	1.7 ± 0.01	1.57 ± 0.01
C20:0	0.21 ± 0.01	0.18 ± 0.01
ΣTFA	0.31 ± 0.02	0.38 ± 0.02
ΣSFA	53.40 ± 1.89	53.25 ± 0.98
ΣMUFA <sup>c</sup>	27.80 ± 0.88	27.96 ± 0.75
ΣPUFA <sup>d</sup>	20.18 ± 0.81	20.02 ± 0.85

<sup>a</sup> Values show the means ± standard deviations. <sup>b</sup> Abbreviations used: 8:0, octanoic acid; 10:0, decanoic acid; 12:0, lauric acid; 14:0, myristic acid; 16:0, palmitic acid; 18:0, stearic acid; 18:1, oleic acid; 18:1t, *trans*-oleic acid; 18:2, linoleic acid; 18:2t, *trans*-linoleic acid; 18:3, linolenic acid; 20:0, arachidic acid. <sup>c</sup> MUFA: mono-unsaturated fatty acid. <sup>d</sup> PUFA: poly-unsaturated fatty acid.

due to its high crystallization rate and low SFC at high temperature which endowed good melting taste.<sup>19</sup> Meanwhile, negligible *trans* fatty acids (TFA) were detected in both A and B samples which was beneficial to develop healthy margarine.

TAG plays a crucial role in the physicochemical properties and the functionality of ISM. The TAGs of the two products were compared as presented in Table 3. The major tri-saturated (S<sub>3</sub>) TAG in two products were 1,2,3-tripalmitoyl glycerol (PPP) (17.42% and 9.89% for A and B, respectively) and 1,2-dipalmitoyl-3-stearoyl glycerol (PPS) (1.08% and 2.09% for A and B, respectively). Di-saturated-mono-unsaturated (S<sub>2</sub>U) TAG were POP (23.83% and 15.87% for A and B, respectively) and POS (3.21% and 2.71% for A and B, respectively). The representative mass spectrum has been provided in the ESI Materials Fig. S2.† Both PPP and POP contents in sample B were relatively lower than that of A because the former contained chemical interesterification (CIE) fat which rearranged TAG. Similar results were reported by Hu *et al.*<sup>19</sup> Overall, compared with A, B exhibited decreased content of S<sub>3</sub> TAG and tri-unsaturated (U<sub>3</sub>) TAG content while increased content of the monosaturated-diunsaturated (SU<sub>2</sub>) TAG. As reported in previous studies, S<sub>3</sub> TAGs can provide a skeleton of a crystal network, and S<sub>2</sub>U and SU<sub>2</sub> TAGs contribute to the lubricity of a fat crystal system. Among them, these high melting TAG provide products with an improved structure and crystallization network.<sup>20</sup> These changes in TAG profiles greatly influenced the physical properties, such as SFC, DSC, polymorphism, hardness, bending and sheeting properties of the samples which will be discussed later.

## 3.2 SFC of the products

SFC plays an important role in product characteristics, including the appearance properties (consistency) and physical



Table 3 Triacylglycerol comparison (%) of samples A and B<sup>a</sup>

TAGs	A	B
C30	0.26 ± 0.01	0.19 ± 0.01
C32	1.21 ± 0.01	0.34 ± 0.01
C34	1.57 ± 0.02	0.33 ± 0.01
C36	3.99 ± 0.09	1.00 ± 0.01
C38	3.24 ± 0.03	1.95 ± 0.01
C40	1.86 ± 0.02	2.16 ± 0.04
C42	1.49 ± 0.01	3.03 ± 0.03
C44	1.15 ± 0.01	5.40 ± 0.43
MPP	1.36 ± 0.01	2.09 ± 0.02
MOM	0.74 ± 0.01	4.29 ± 0.67
PPP	17.42 ± 1.01	9.89 ± 0.01
MOP	1.53 ± 0.05	2.42 ± 0.04
MLP	0.80 ± 0.01	2.86 ± 0.03
PPS	1.08 ± 0.01	2.09 ± 0.01
POP	23.83 ± 0.87	15.87 ± 0.32
MOO	0.47 ± 0.01	0.39 ± 0.01
PLP	5.04 ± 0.23	7.84 ± 0.21
MLO	0.30 ± 0.01	0.66 ± 0.01
PSS	0.33 ± 0.01	0.36 ± 0.01
POS	3.21 ± 0.03	2.71 ± 0.02
POO	8.45 ± 0.07	6.78 ± 0.07
PLS	1.19 ± 0.03	1.88 ± 0.02
PLO	5.14 ± 0.02	8.35 ± 0.03
PLL	3.34 ± 0.02	3.58 ± 0.01
SSS	0.24 ± 0.03	0.18 ± 0.01
SOS	0.84 ± 0.01	0.70 ± 0.01
SOO	1.56 ± 0.03	1.17 ± 0.02
OOO	0.80 ± 0.01	0.82 ± 0.01
SLO	2.45 ± 0.04	2.26 ± 0.05
OLO	2.64 ± 0.03	1.65 ± 0.01
OLL	2.47 ± 0.03	0.62 ± 0.01
ΣU <sub>3</sub>	5.91 ± 0.13	3.09 ± 0.12
ΣSU <sub>2</sub>	20.65 ± 0.72	29.33 ± 0.97
ΣS <sub>2</sub> U	37.18 ± 1.55	38.57 ± 1.87
ΣS <sub>3</sub>	36.26 ± 1.23	29.01 ± 1.76

<sup>a</sup> Abbreviation: TAGs: triacylglycerols; P, palmitic acid; La, lauric acid; L, linoleic acid; Ln, linolenic acid; O, oleic acid; M, myristic acid; S, stearic acid; A, arachidic acid; U<sub>3</sub>, tri-unsaturated TAG; SU<sub>2</sub>, di-unsaturated TAG; S<sub>2</sub>U, monounsaturated TAG; S<sub>3</sub>, tri-saturated TAG. XXY, YXX, XXX and XYZ represent structures of triacylglycerols, for example, POS stands for the structure of 1/3-palmitoyl-2-oleoylglycerol-1/3-stearoyl.

properties (ductility and fusibility) of margarine and shortening.<sup>21</sup>

The variation ranges and slope degrees of SFC curves determine whether the fat meets the requirements. In general, sheet margarine containing 10–40% solid fat within the

temperature range of 10–33.3 °C enables a better temperature tolerance.<sup>14,22</sup> Fig. 1 displays the curves of SFC as a function of temperature for oil base (a) and ISM (b and c). As seen in Fig. 1(a), the SFC of B is lower than A at temperatures of 20 to 40 °C while higher at 10 °C exhibiting a slightly steeper SFC curve. This was mainly due to their different TAG compositions. The lower SFC at 40 °C (~5%) for B endowed it better melting taste which was a good benefit for ISM application.

The SFC of ISM decreased with increasing tempering temperature as shown in Fig. 1(b and c). For ISM stored at 10 °C, the SFC decreased from 38.68% to 30.60% for sample A and 40.77% to 33.13% for sample B tempered from 10 °C to 30 °C. Similarly, the SFC decreased from 28.29% to 18.95% for sample A and 28.87% to 18.06% for sample B tempered from 10 °C to 30 °C when stored at 20 °C. However, the decline degree of A was smaller than that of B which may due to A contained more content of high melting TAGs (S<sub>3</sub>) and less content of lower melting TAGs (SU<sub>2</sub>). S<sub>3</sub> can be solid weather at low temperature or high temperature while SU<sub>2</sub> may be solid at low temperature but may melt with increasing tempered temperature. The different content of various melting point TAGs leads to different slopes of the SFC curve, presenting consistency with the previous report.<sup>23</sup> The SFC of ISM products was lower than their corresponding oil bases and varied with tempering temperature which was mainly due to their different crystallization process. Therefore, the properties of ISM were greatly influenced by tempering temperature although they have the same oil base SFC.

### 3.3 Microstructures observed by PLM

A polarized light microscope (PLM) is commonly adopted to evaluate the characterization and the microstructures of crystallization. The crystal morphology of products A and B tempered at 10 °C, 15 °C, 20 °C, 25 °C, and 30 °C respectively was observed by PLM. Under PLM, fat crystals are bright due to the birefringence of fat crystals.<sup>21</sup> The particle size of the crystal has a significant influence on the application of the final product. Small crystals can improve the hardness of the product, but large crystals would lead to a sandy texture.<sup>24</sup> Tempering temperature had a great impact on the quantity, type of crystal, and stability of the crystal network.

Fig. 2 revealed the gradual increment in the number of crystals with increasing tempering temperature and the number of crystals decreased once the tempering temperature was above

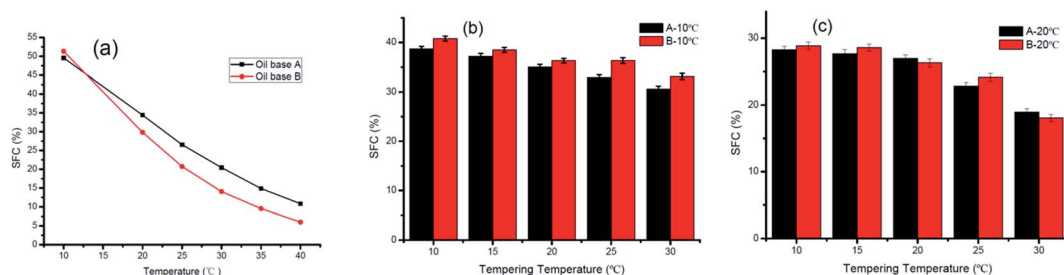


Fig. 1 SFC of an oil base (a), SFC of products A and B at 10 °C (b) and 20 °C (c) under different tempering conditions.



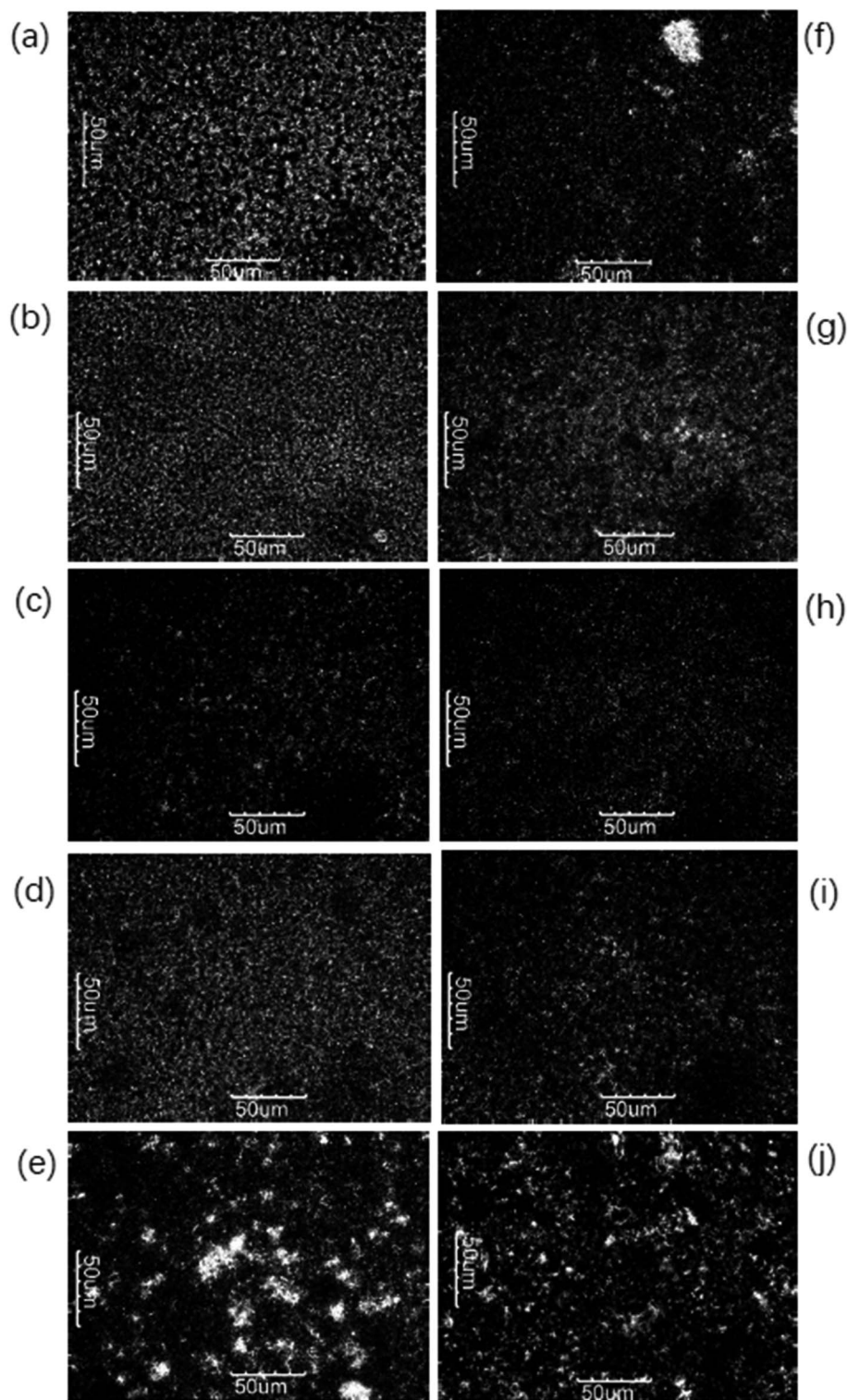


Fig. 2 Crystal morphologies of A (a–e) and B (f–j) tempered at 10 °C, 15 °C, 20 °C, 25 °C, and 30 °C, respectively.

25 °C, mainly caused by the melting of low melting point components (POO, SOO). The modification of crystal types from different tempered temperatures can be demonstrated in combination with XRD. The tempering process is favored to form a stable crystal network structure, but the increased

tempering temperature can loosen the crystal network and decrease the quality of the final product.

PLM images also demonstrated the more uniform and smoother crystal structure of product A and had a finer crystalline state along with the increasing tempering temperatures



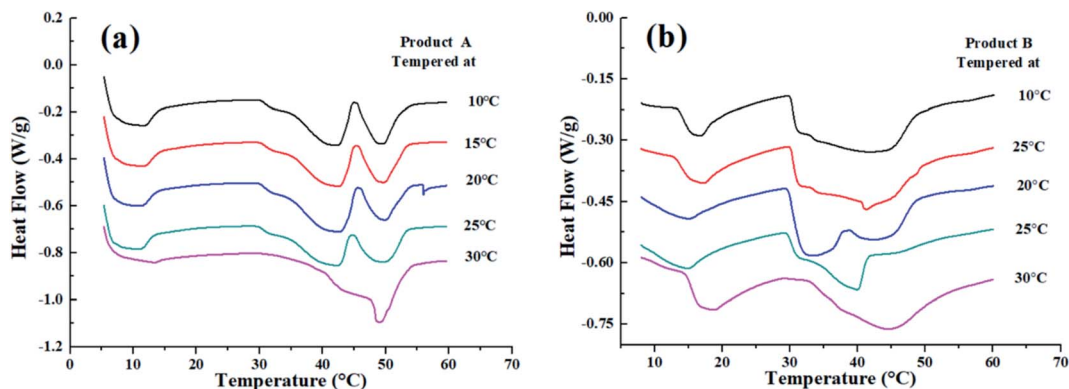


Fig. 3 DSC curves of A and B tempered at 10 °C, 15 °C, 20 °C, 25 °C, and 30 °C.

within 25 °C. After being tempered at 20 °C and 25 °C, the microstructure of the product was better than tempered below 20 °C. Noteworthy, the effect of product B was not obvious as compared to product A.

### 3.4 Thermal behaviors by DSC

The melting behaviors of products A and B changed greatly after being tempered at different temperatures. For product B, after tempered at 10 °C, 15 °C, 20 °C, and 25 °C, a larger melting peak was exhibited at around 35 °C compared with the previous non-CIE one. These results suggested the partial disintegration of the mixed TAG, which is linked with the crystal type transmutation from  $\beta'$  to  $\beta$  form during the tempering process. A single melting peak was presented at 45 °C while tempering at 30 °C, indicating the transition acceleration of  $\beta'$  into  $\beta$  crystals at higher tempering temperature as evidenced by the XRD results. However, for product B which contains CIE fat, the number of peaks did not change despite being tempered at different temperatures (except 20 °C). Nevertheless, from the melting curve, the delayed-melting peak indicated a more uniform TAG distribution in the CIE formula. The aforementioned results concluded that the tempering process contributed to the stability of the product (Fig. 3).

### 3.5 The rate of crystallization

Fig. 4 showed the SFC vs. time curve of oil base A and B at different crystallization temperatures.

For most conditions, oil base A had a faster crystallization rate than B which may be due to B had lower contents of PPP, POP, and POS when it contained CIE fat. Similar results were reported by Zhang *et al.*<sup>25</sup> They found that the crystallization rate of 50% POL + 50% SheaOL25 was delayed after CIE. The crystallization rate was very fast in the initial 2 min, then experienced a trend of decreasing, increasing, and decreasing, namely the S-shaped curve for both A and B with the prolongation of time. The crystallization rate decreased gradually with the increase in crystallization temperature.

Oil base A presented a faster initial crystallization rate than oil base B which may be due to its high content of PPP, POP and

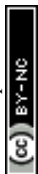
POS. Therefore, A may reach supersaturation state earlier than B at the initial crystallization stage. Similar time was taken for the two products to reach crystallization equilibrium, but both took lesser time to achieve the equilibrium as the temperature increased.

### 3.6 Polymorphic behaviors

The functionalities of products were largely determined by the polymorphism, crystal habit, crystal number, and size.<sup>26,27</sup>  $\alpha$  (peak at 4.15 Å),  $\beta'$  (peak at 4.2–4.3 Å and 3.7–4.0 Å), and  $\beta$  (peak at 4.6 Å) are three major polymorphic types in fats,<sup>14</sup> which are arranged in ascending order of melting point, aggregation density, thermal resistant stability and can be determined by wide-angle XRD. Polymorphism was identified according to the previous research.<sup>28,29</sup> The XRD curves of the samples tempered at different temperatures are displayed in Fig. 5.

Sample A tempered at 10, 15, 20 or 25 °C exhibited strong peaks around 3.8 Å, 4.2–4.3 Å and weak peak at 4.6 Å while tempered at 30 °C showed very strong peak at 4.6 Å as presented in Fig. 5(a). This indicated that sample A was mainly  $\beta'$  form when tempered at 10, 15, 20 or 25 °C but transformed into  $\beta$  form when tempered at 30 °C.

An entirely different phenomenon was displayed in sample B in Fig. 5(b), which presented the strong  $\beta$  form diffractions at all tempering temperatures with varying intensity of  $\beta$  forms. The tempering at 20 °C and 25 °C resulted in the relatively strong  $\beta'$  diffraction appearing near 4.2 Å, implying that the conversion of  $\beta'$  to  $\beta$  was retarded at 20 °C and 25 °C tempering temperatures. Nevertheless, the polymorph transition ( $\beta' \rightarrow \beta$ ) was monitored as the tempering temperature increased. The sample tempered at 30 °C displayed a higher prevalence of  $\beta$  form which has a poor spread-ability for sheet margarine.<sup>30,31</sup> Sample B tempered with increasing temperatures showed less strength of polymorphism conversion partially because of less PPP content due to the CIE formulation despite similar polymorphism with sample A. Moziar *et al.* also found that the  $\beta'$  form of shortening tends to transform to more stable  $\beta$  form at 30 °C.<sup>8</sup> Similar results were found by Aini *et al.* and the transition extent sometimes depended on the oil base.<sup>32</sup>



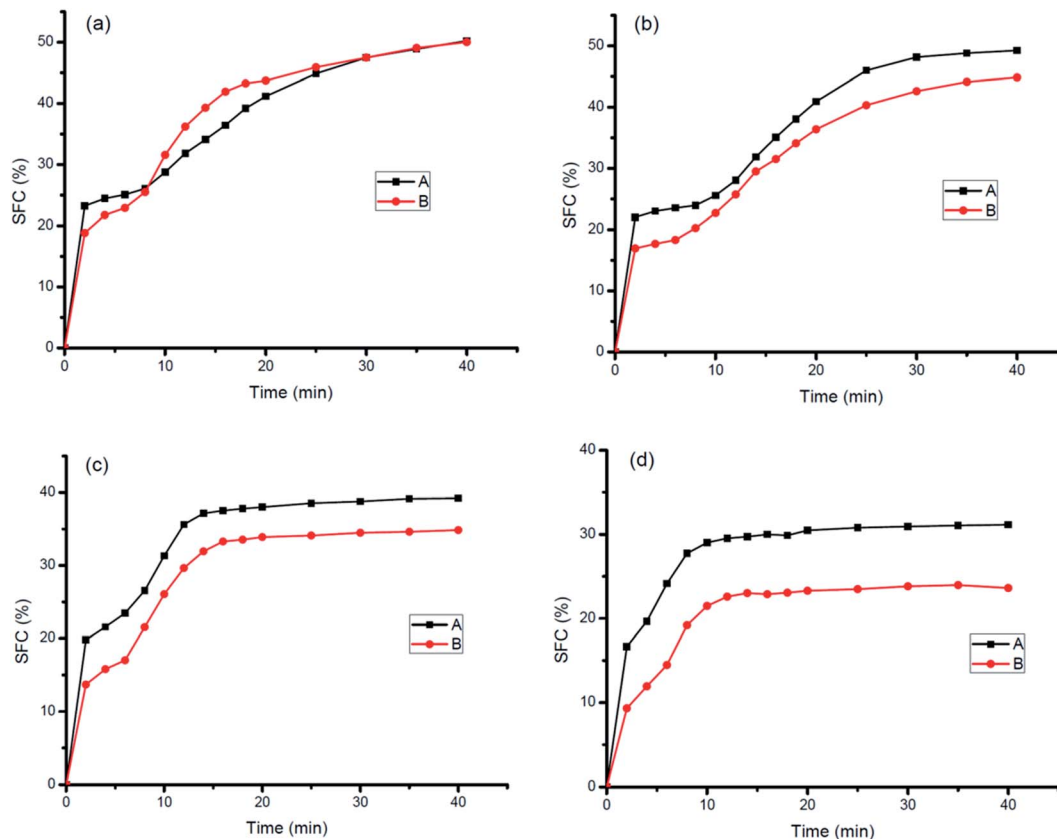


Fig. 4 Crystallization rate of samples A and B at 5 °C (a), 10 °C (b), 15 °C (c), and 20 °C (d).

In this study, the polymorph of A and B completely turned to  $\beta$  form when tempered at 30 °C with large crystals shown in Fig. 2(e) and (j) and this greatly influenced their application property (bad bending and sheeting properties) showed in Fig. 7 and 8. The correspondence between the different crystalline forms and the sheeting properties was presented in ESI Fig. S3.†

### 3.7. Hardness and textural properties

The hardness of sheet margarine mainly relies on the SFC, crystallization forms, and triacylglycerol compositions.<sup>33–35</sup>

Hardness imparts detailed information on the workability, functionality, and sensory properties of products and significantly contributes to practical application.<sup>34</sup> Fig. 6 shows the change in hardness of products A and B tempered at various temperatures.

The hardness of samples decreased as temperature increased which may be due to the decreased SFC as shown in Fig. 1(a). For sample A, its hardness varied with tempering temperatures shown in Fig. 6(a). The hardness decreased when tempering temperature increased from 15 °C to 25 °C but

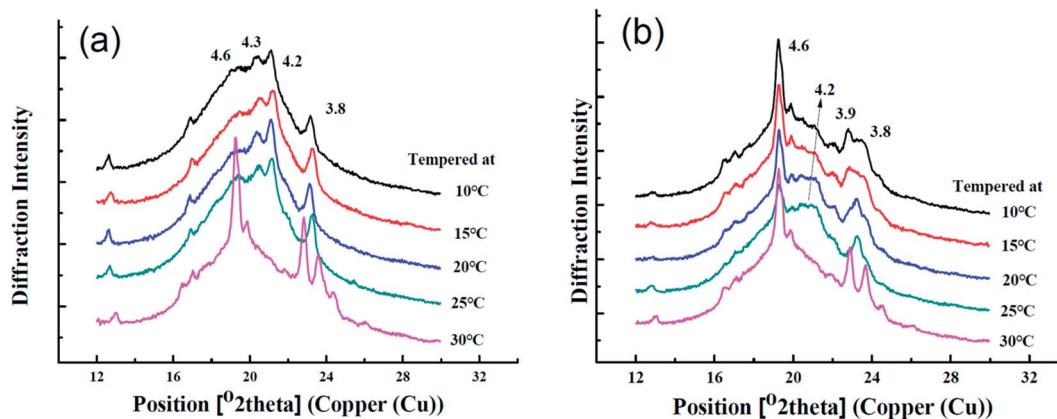


Fig. 5 XRD of samples A and B tempered at 10 °C, 15 °C, 20 °C, 25 °C, and 30 °C.





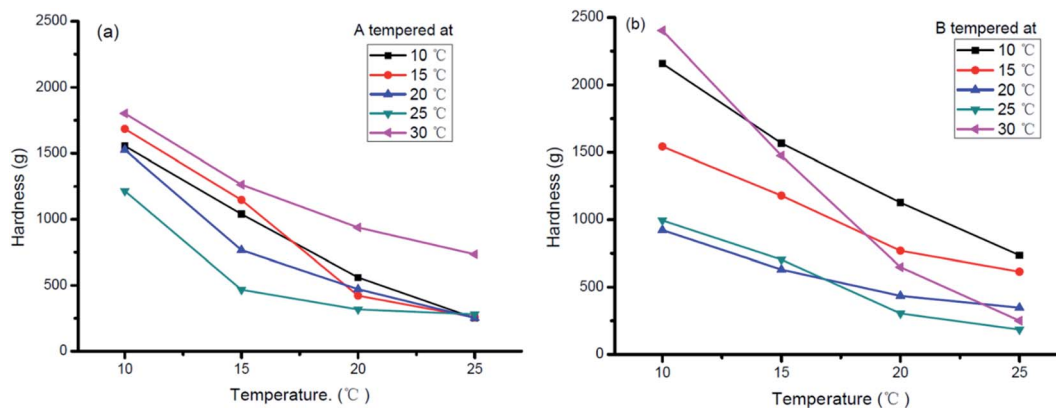


Fig. 6 The hardness of A and B tempered at 10 °C, 15 °C, 20 °C, 25 °C, and 30 °C.

increased greatly when tempered at 30 °C. Taking the samples stored at 20 °C for 24 hours as an example, the hardness value reached 700 g for sample tempered at 30 °C but only about 300 g for those tempered at other temperatures. The decrease in hardness may be mainly due to the decreasing SFC content as shown in Fig. 1(b) and (c) while the increase in hardness tempered at 30 °C was mainly due to the  $\beta$  morphology conversion as shown in Fig. 5(a). Sample B showed similar hardness variation at different tempering temperatures (Fig. 6(b)). It was more significantly affected by the storage temperature except for 25 °C and 30 °C tempered products. In addition, appropriate hardness (between 400 and 500 g) of sample B was obtained after tempered at 25 °C, which satisfied the hardness requirement of commercial sheet margarine.<sup>36</sup>

### 3.8. Bending and sheeting properties

Three key performance characteristics of sheet margarine are described as firmness (consistency), plasticity, and melting

properties by several researchers.<sup>37,38</sup> Excellent sheet margarine must be hard and flexible enough to tolerate the high intensity of shear and pressure exerted during the rolling and to achieve continuous unbroken thin fat layers.

As shown in Fig. 7, the fractures of different samples at 90° folding were evaluated. The optimum bending effect of sample A was achieved under the tempering temperature of 20 °C and 25 °C but displayed inferior properties at low tempering temperatures (10 °C and 15 °C) and high tempering temperatures (30 °C). Sample B also showed a similar trend but its fracture surface was coarser than sample A at the same tempering temperature. The sheeting properties of samples A and B at different tempering temperatures were evaluated as shown in Fig. 8. Samples A and B displayed tendencies to break and form rough fat layers when tempered at high (30 °C) and low (10 °C and 15 °C) temperatures due to their hard and brittle characteristics. Nevertheless, both samples tempered at 20 °C and 25 °C produced smooth continuous fat bands while

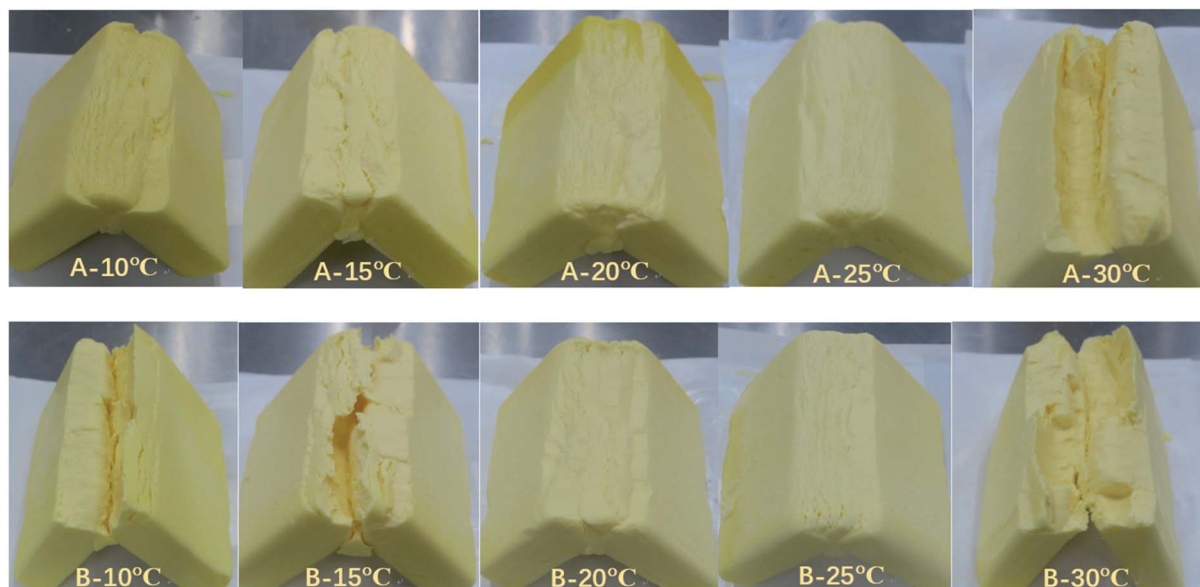


Fig. 7 Bending test of samples tempered at 10 °C, 15 °C, 20 °C, 25 °C, and 30 °C.



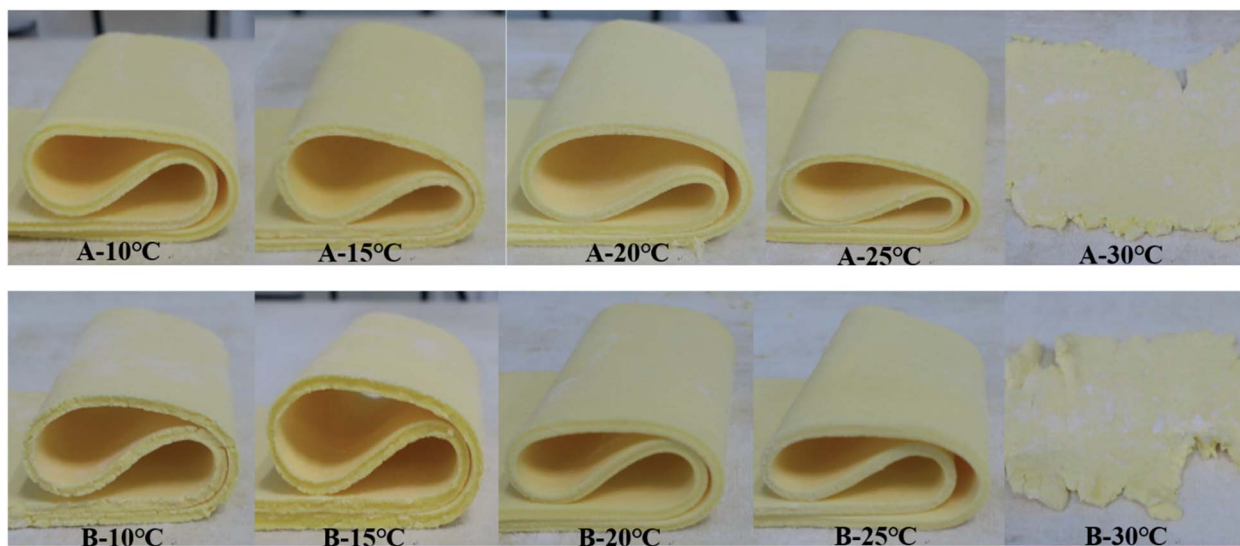


Fig. 8 Sheeting abilities of samples A and B tempered at different temperatures (10 °C, 15 °C, 20 °C, 25 °C, and 30 °C).

sheeting. The results indicated the effect of tempering temperatures of 20 °C and 25 °C on optimum plasticity and sheet properties.

## 4 Conclusions

The physical and applicational properties of two typical commercial formulated ISMs under different tempering temperatures were characterized based on SFC, thermal stability, hardness, crystal morphology, bending and sheeting abilities. It was found that ISMs tempered at 10 °C and 15 °C had relatively good thermal stability with a dominated  $\beta'$  crystal type, but the higher SFC value (more than 28%), the denser morphology and the significantly increased values for hardness which most likely due to the formation of primary bonds leading to bad bending and sheeting abilities. Samples tempered at 30 °C showed significantly increased hardness also led to the poor ductility which resulted from crystallization transformation to  $\beta$ . Therefore, too low/high tempering temperatures can deteriorate the practical operational properties. Compared to the above high hardness, moderate hardness is obtained and both samples presented finer and more uniform crystalline through tempering at 20 °C and 25 °C. The products tempered at 20 °C and 25 °C exhibited better-bending properties and spreadability which can be beneficial for bakery product applications. The results provided a meaningful theoretical guidance for the subsequent industrial production of ISM.

## Author contributions

Houbin Gao: writing – original draft, methodology, data curation, conceptualization. Wei Gao: visualization, data curation. Xiaoming Yang: formal analysis, validation. Yuanfa Liu: conceptualization, methodology. Zhouping Wang: conceptualization, supervision, writing-review & editing.

## Conflicts of interest

There are no conflicts of interest to declare.

## Acknowledgements

The author gratefully acknowledged Dr Chunhuan Liu (Jingnan University) for her useful discussion and assistance.

## References

- 1 B. S. Ghotra, S. D. Dyal and S. S. Narine, *Food Res. Int.*, 2002, **35**, 1015–1048.
- 2 V. Nguyen, T. Rimaux, V. Truong, K. Dewettinck and F. Van Bockstaele, *Cryst. Growth Des.*, 2020, **20**, 1363–1372.
- 3 T. J. Silva, D. Barrera-Arellano and A. P. B. Ribeiro, *Food Res. Int.*, 2021, **147**, 110486.
- 4 N. Viet, T. Rimaux, T. Vinh, K. Dewettinck and F. Van Bockstaele, *J. Food Eng.*, 2021, **291**, 110–124.
- 5 R. Campos, S. S. Narine and A. G. Marangoni, *Food Res. Int.*, 2002, **35**, 971–981.
- 6 C. W. Chen, C. L. Chong, H. M. Ghazali and O. M. Lai, *Food Chem.*, 2007, **100**, 178–191.
- 7 N. Drelon, E. Gravier, L. Daheron, L. Boisserie, A. Omari and F. Leal-Calderon, *Int. Dairy J.*, 2006, **16**, 1454–1463.
- 8 C. Moziar, J. M. deMan and L. deMan, *Can. Inst. Food Sci. Technol. J.*, 1989, **22**, 238–242.
- 9 Z. M. Zhang, H. Zhang, B. I. Yan-Lan, X. Y. Sun and X. Xue-Bing, *J. Food Sci.*, 2013, **1**, 111–117.
- 10 B. A. Macias-Rodriguez, R. H. Ewoldt and A. G. Marangoni, *Rheol. Acta*, 2018, **57**, 251–266.
- 11 Q. Zhou, B. Gao, X. Zhang, Y. Xu, H. Shi and L. Yu, *Food Chem.*, 2014, **143**, 199–204.
- 12 R. Detry, V. Van Hoed, J. Sterckx, C. Deledicque, K. Sato, C. Blecker and S. Danthine, *Eur. J. Lipid Sci. Technol.*, 2020, **123**, 1556–1563.



- 13 X. Chai, Z. Meng, J. Jiang, P. Cao, X. Liang, M. Piatko, S. Campbell, S. K. Lo and Y. Liu, *Food Res. Int.*, 2018, **105**, 423–431.
- 14 B. S. Ghotra, S. D. Dyal and S. S. Narine, *Food Res. Int.*, 2002, **35**, 1015–1048.
- 15 G. Pande, C. C. Akoh and R. L. Shewfelt, *Biocatal. Agric. Biotechnol.*, 2013, **2**, 76–84.
- 16 V. De Graef, J. Vereecken, K. W. Smith, K. Bhaggan and K. Dewettinck, *Eur. J. Lipid Sci. Technol.*, 2012, **114**, 592–601.
- 17 A. G. Marangoni, J. P. M. van Duynhoven, N. C. Acevedo, R. A. Nicholson and A. R. Patel, *Soft Matter*, 2020, **16**, 289–306.
- 18 S. B. A. Lounis, L. Mekimene, D. Mazi, T. Hamidchi, S. Hadjal, S. Boualit and M. Benalia, *Mediterr. J. Nutr. Metabol.*, 2018, **11**, 331–342.
- 19 Hu Peng, X. Xu and L. Yu, *LWT–Food Sci. Technol.*, 2017, **76**, 156–163.
- 20 V. Nguyen, T. Rimaux, V. Truong, S. Danthine, K. Dewettinck and F. Van Bockstaele, *J. Am. Oil Chem. Soc.*, 2020, **98**, 115–125.
- 21 S. Can, C. Ming, L. Ruijie, J. Qingzhe and W. Xingguo, *Int. J. Food Eng.*, 2015, **11**, 467–477.
- 22 A. J. Haighton, *J. Am. Oil Chem. Soc.*, 1959, **36**, 345–348.
- 23 P. Garcia-Macias, M. H. Gordon, R. A. Frazier, K. Smith and L. Gambelli, *Eur. J. Lipid Sci. Technol.*, 2012, **114**, 741–747.
- 24 X. Zhang, L. Li, H. Xie, Z. Liang, J. Su, G. Liu and B. Li, *Food Bioprocess Technol.*, 2014, **7**, 887–900.
- 25 Z. Zhang, X. Ma, H. Huang and Y. Wang, *LWT–Food Sci. Technol.*, 2017, **86**, 492–500.
- 26 B. Macias-Rodriguez and A. G. Marangoni, *J. Am. Oil Chem. Soc.*, 2016, **93**, 575–585.
- 27 C. Liu, Z. Meng, X. Chai, X. Liang, M. Piatko, S. Campbell and Y. Liu, *Food Chem.*, 2019, **286**, 636–643.
- 28 Y. Shimomura, M. Tsuchiya, S. Ueno and M. Shiota, *J. Am. Oil Chem. Soc.*, 2019, **96**, 35–42.
- 29 V. Nguyen, T. Rimaux, V. Truong, K. Dewettinck and F. V. Bockstaele, *J. Food Eng.*, 2021, **291**, 110–124.
- 30 M. Kellens, W. Meeussen and H. Reynaers, *J. Am. Oil Chem. Soc.*, 1992, **69**, 906–911.
- 31 A. G. Marangoni and S. E. Mcgauley, *J. Cryst. Growth*, 2002, **3**, 95–108.
- 32 I. N. Aini, N. Widlak, R. Hartel and S. Narine, *Crystallization and solidification properties of lipids*, 2001, pp. 42–52.
- 33 B. Pajin, D. Šoronja-Simović, Z. Šereš, J. Gyura, I. Radujko and M. Sakač, *Eur. J. Lipid Sci. Technol.*, 2011, **113**, 262–268.
- 34 L.-Z. Cheong, C.-P. Tan, K. Long, M. S. A. Yusoff and O.-M. Lai, *J. Sci. Food Agric.*, 2010, **90**, 2310–2317.
- 35 Y. Shimomura, M. Tsuchiya, S. Ueno and M. Shiota, *J. Am. Oil Chem. Soc.*, 2019, **96**, 35–42.
- 36 R. Detry, V. Van Hoed, J. Sterckx, C. Deledicque, K. Sato, C. Blecker and S. Danthine, *Eur. J. Lipid Sci. Technol.*, 2015, **117**, 1687–1699.
- 37 P. Wassell and N. W. G. Young, *Int. J. Food Sci.*, 2007, **42**, 503–517.
- 38 Q. Zhou, *et al*, *Food Chem.*, 2014, **143**, 199–204.

